

# Spatio-temporal Assessment of Soil Erosion Risk in the Tono River Basin, Upper East Ghana, using the RUSLE Model

Abdullah Alhassan<sup>1\*</sup>, Jawal Sualisu<sup>1</sup>, Abdul-Kadri Yahaya<sup>1</sup>

<sup>1</sup>Department of Environment and Resource Studies, Faculty of Integrated Development Studies, University of Business and Integrated Development Studies (UBIDS), XW-1147-8901, Bamahu-Wa, Ghana; [aalhassan@ubids.edu.gh](mailto:aalhassan@ubids.edu.gh)

\* Corresponding author

DOI: <https://dx.doi.org/10.4314/sajg.v15i1.1>

## Abstract

*This study presents a comprehensive assessment of soil erosion dynamics in the Tono River Basin, Upper East Ghana, from 2017 to 2024, employing the Revised Universal Soil Loss Equation (RUSLE) in combination with geospatial technologies and statistical analysis. The research reveals a dramatic 217.1% increase in mean soil erosion rates, escalating from 0.85t/ha/yr to 2.68t/ha/yr, with total annual soil loss surging from 8.27 to 26.24 million tons. Spatial analysis demonstrated significant clustering of erosion patterns, with Global Moran's I increasing from 0.189 to 0.259, indicating strengthened spatial organization of erosion hotspots over time. Land use change analysis revealed complex erosion responses, including a paradoxical 244.1% erosion increase in the expansion of forested areas (131.9% growth) and an extraordinary 5,023.7% erosion escalation in fragmented flooded vegetation zones. The study identified persistent erosion hotspots covering 24.3% of the basin, alongside emerging hotspots (10.8%) and recovered areas (10.2%). Factor correlation analysis showed topography (LS factor) as the primary control ( $r = 0.756$ ), while vegetation cover factors substantially increased in importance. The findings underscore the critical need for targeted conservation strategies to address the specific erosion processes and the identified spatial patterns, to provide a scientific foundation for sustainable land management in semi-arid watersheds experiencing rapid environmental change.*

## 1. Introduction

Soil erosion is a critical form of land degradation that threatens agricultural productivity, food security, and environmental sustainability on a global scale (Borrelli *et al.*, 2017; Lal, 2001). It acts as a catalyst to several environmental problems, including decreased land productivity, challenges to agricultural sustainability, and degradation of soil and water quality (Dumedah & Evans Kyeremanteng, 2019). In arid and semi-arid regions, such as those in sub-Saharan Africa, this problem is particularly acute. These ecosystems are characterized by fragile soils, intense but highly variable rainfall, and increasing anthropogenic pressure from activities such as deforestation, unsustainable farming practices, and uncontrolled grazing (Adongoa *et al.*, 2019; Vrieling, 2006). The loss of fertile topsoil directly reduces the capacity of the land to support vegetation, leading to a vicious cycle of declining yields, increased

poverty, and further land exploitation (Bai *et al.*, 2008). This is a global concern, with an estimated 10 million hectares of cropland lost to soil erosion annually (Brown, 2019). (Ghosh *et al.*, 2022) emphasize that soil erosion is a significant global problem contributing to nutrient loss, water quality degradation, and sand accumulation, with agricultural intensification and soil degradation being the key drivers.

Tono River Basin in northern Ghana is a quintessential example of a region facing these interconnected challenges. As a vital area for agriculture and water supply — in that it hosts the Tono Reservoir, with a storage capacity of 93 million cubic metres — its success as a key water source is crucial for local livelihoods and regional food security (Adongoa *et al.*, 2019; Alhassan & Jin, 2020). The climatic region into which the basin falls can be differentiated into distinct rainy (July–September) and dry (December–February) seasons, with the mean annual precipitation varying between 700 and 1100 mm. However, owing to its climatic conditions and evolving land use patterns, it is inherently vulnerable to erosion. In Ghana's Upper East Region, a neighbouring area with similar ecological pressures, soil erosion has been identified as a leading cause of land degradation, loss of soil fertility, and food insecurity (Sodoke *et al.*, 2025). Furthermore, climate change is projected to increase the intensity of rainfall events in the region, thereby potentially accelerating erosion rates (Nkrumah *et al.*, 2019). Concurrently, population growth and agricultural expansion are altering the land cover, often reducing the natural vegetation that protects the soil. (Adongoa *et al.*, 2019) noted that cropland, which has a high potential for erosion, constitutes a predominant form of land use in the reservoir catchments of northern Ghana. Recent land cover analyses of the Tono Basin itself have documented significant land use /land cover changes, including a substantial expansion of shrubland and a contraction of forest and cropland/agroforestry areas between 2009 and 2017 (Alhassan & Jin, 2020), transformations that can profoundly influence soil erosion dynamics.

Recent studies, such as that by (OSEI-GYABAAH *et al.*) of the Asutifi North District, further confirm that factors such as deforestation, a decline in the vegetation cover, and unsustainable farming practices are key drivers of the rising soil erosion rates in Ghana. Understanding the spatial distribution and temporal dynamics of soil loss in such basins is the first step toward developing effective conservation strategies, a point also underscored by (Ganasri & Ramesh, 2016).

Empirically-based models have become indispensable tools for quantifying soil erosion risk over large areas. The Revised Universal Soil Loss Equation (RUSLE) is one of the most widely applied and robust models for predicting average annual soil loss from sheet and rill erosion (Panagos *et al.*, 2015; Renard, 1997). Its strength lies in its ability to integrate the key factors governing erosion — rainfall erosivity (R), soil erodibility (K), topography (LS), land cover management (C), and conservation practices (P) — into a spatially explicit framework (Dumedah & Evans Kyeremanteng, 2019; Mantey & Aduah, 2020). The RUSLE model has

been applied widely across Ghana to estimate soil loss and, on account of its highly predictive accuracy, has proven effective (Sodoke *et al.*, 2025). (Ganasri & Ramesh, 2016) highlight that modelling provides a quantitative and consistent approach to estimating soil erosion under a wide range of conditions. The advantages of RUSLE include its simplicity of use, the ease of interpretation of the data generated, and its reliance on factors that are manageable to map-using GIS tools and detectable by satellite remote sensing. (Abdelsamie *et al.*, 2022) further note that integrating RUSLE with GIS and remote sensing establishes a scientific and accurate method to calculate the extent of soil erosion. While the traditional application of RUSLE was data-intensive and limited to small plots, the advent of cloud-computing platforms such as Google Earth Engine (GEE) has revolutionized its implementation (Gorelick *et al.*, 2017; Tamene & Le, 2015). Studies in Ghana are increasingly leveraging GEE for tasks such as image downloading, processing, and calculating annual soil erosion rates which together provide a long-term, high-resolution dataset crucial for capturing spatial and temporal variability (OSEI-GYABAAH *et al.*; Sodoke *et al.*, 2025). GEE provides seamless access to vast sources of satellite imagery and geophysical datasets, enabling the efficient, large-scale computation of all RUSLE factors at high resolution.

Previous studies in Ghana and neighbouring regions have highlighted significant soil erosion hazards (Adongoa *et al.*, 2019; Mantey & Aduah, 2020; Nyamekye *et al.*, 2018). For instance, in the Asokore Mampong Municipality, soil loss was estimated to be as high as 440 t ha<sup>-1</sup> yr<sup>-1</sup> (Dumedah & Evans Kyeremanteng, 2019), while reservoir catchments in northern Ghana exhibited rates that in some cases exceeded the tolerable limits (Adongoa *et al.*, 2019). Recent research by (Sodoke *et al.*, 2025) in the Upper East Region recorded average annual soil loss rates far exceeding the acceptable tolerance limits, with values of 50.26 and 56.50 t ha<sup>-1</sup> yr<sup>-1</sup> for different periods, underscoring the severity of the threat. Similarly, (OSEI-GYABAAH *et al.*) reported a mean soil loss of 27.65 t ha<sup>-1</sup> yr<sup>-1</sup> in the Asutifi North District, with some areas experiencing severe erosion above 40 t ha<sup>-1</sup> yr<sup>-1</sup>. These findings align with global studies; for example, (Ghosh *et al.*, 2022) reported an annual soil loss of 4.6 million tons in the Mayurakshi River Basin, while (Ganasri & Ramesh, 2016) estimated 473,339 t/yr in the Nethravathi Basin. Furthermore, research within the Tono Basin itself has highlighted the impact of land use on sedimentation in the Tono Reservoir, directly linking land degradation to water resource management challenges. However, many of these assessments have been constrained by coarse spatial resolution levels, limited temporal scope, or the use of simplified vegetation indices such as NDVI for the cover management (C) factor, which can be less effective in semi-arid landscapes with high soil background exposure. Sodoke *et al.* (2025) emphasized that cover management (C) and support practices (P) are among the most significant factors impacting soil loss, thereby highlighting the critical need for accurate vegetation and land management data. The Transformed Soil-adjusted Vegetation Index (TSAVI), which accounts for the soil line, offers a more robust alternative for accurately

characterizing vegetation cover in such environments (Baret & Guyot, 1991). The importance of vegetation cover as a crucial factor in preventing soil erosion is well established, and the use of advanced satellite imagery, such as Sentinel-2, which offers high-resolution multi-spectral data, can significantly improve the accuracy of C-factor estimations (Abdelsamie *et al.*, 2022).

This study addresses these gaps by conducting a high-resolution (10m), multi-temporal assessment of soil erosion risk for the Tono Basin for the years 2017 and 2024. We leveraged the power of Google Earth Engine to integrate multi-source data, including CHIRPS, for rainfall, Sentinel-2 for deriving TSAVI-based land cover, SRTM for topography, and global soil grids for erodibility. This approach allowed for a detailed analysis that could build upon the existing understanding of the land cover dynamics of the basin and its role in critical surface processes such as evapotranspiration (Alhassan & Jin, 2020). The integration of Remote Sensing (RS), Geographic Information Systems (GIS), and the RUSLE model provided a powerful basis for assessing current erosion conditions and identifying priority areas for intervention.

The primary objectives of this research were:

- 1) To develop and implement a spatially explicit RUSLE model within the Google Earth Engine platform for the Tono Basin.
- 2) To map and quantify the annual soil loss rates for 2017 and 2024, identifying areas of high and very high erosion risk.
- 3) To analyse the spatial patterns of the individual RUSLE factors (R, K, LS, C, P) to determine the dominant drivers of erosion in the basin.
- 4) To assess the changes in erosion risk between the two time points, linking them to potential changes in land cover and rainfall patterns.

The findings of this study will provide critical, evidence-based insights for land-use planners, soil conservationists, and policymakers in Ghana. By pinpointing erosion hotspots and understanding their causes, this research aims to inform targeted intervention strategies, thereby contributing to the sustainable management of the vital land and water resources of the Tono Basin.

## **2. Materials and methods**

### **2.1. Study area**

The study was conducted in the Tono Basin, located in Upper East Region of Ghana (Fig 1). The basin lies in a semi-arid climate region, with the single rainy season typically occurring between June and October. The area is dominated by agricultural activities, savanna vegetation, and varying topographic conditions, making it susceptible to soil erosion. The predominant soil

types, based on the SoilGrids database used in this analysis, are Luvisols, which cover approximately 80% of the basin and Gleysols (~10%), with the remaining area comprising a mix of Acrisols, Lixisols, and Vertisols.

Geologically, the Tono Basin lies within the vast Voltaian Basin, an inland sedimentary basin formed during the Pan-African Orogeny. The basin is filled with rocks dating back to the Precambrian and to Paleozoic sedimentary rocks, including sandstones, shales, and mudstones, which form the parent material for the soils of the region. The significant thickness of these sediments underscores the deep weathering profiles that influence the present day soil erosion processes. The properties of these sedimentary rocks directly influence soil erodibility (K-factor) and the overall susceptibility of the landscape to the erosion processes quantified in this study.

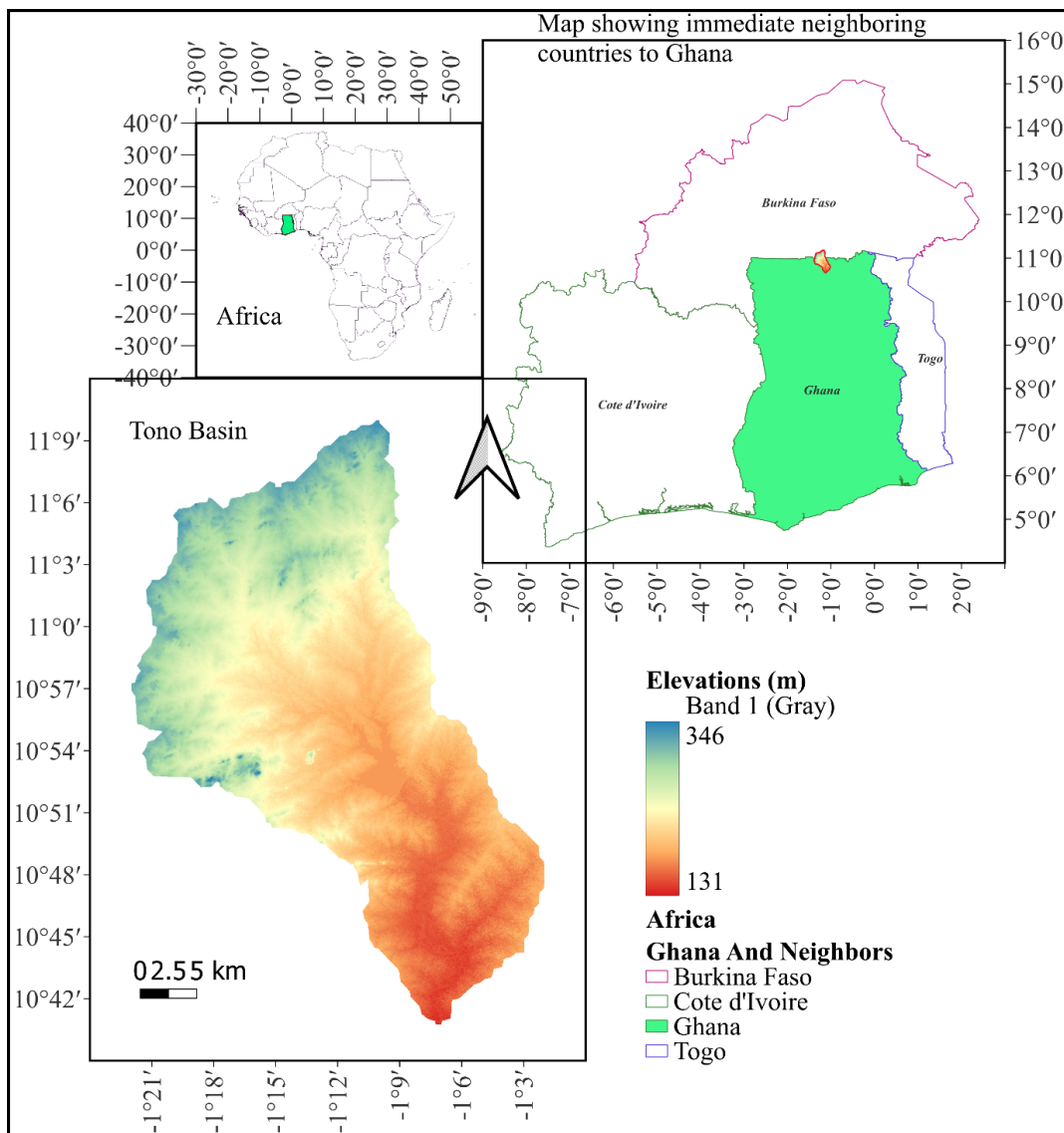


Figure 1. Topographic map of the Tono Basin study area, Upper East Region, Ghana, showing elevation variations and geographical context within Africa

## **2.2. The RUSLE model**

Soil loss was estimated using the Revised Universal Soil Loss Equation (RUSLE), which is an empirical model designed to predict long-term average annual soil loss. The model is expressed as:

$$A = R \times K \times L \times S \times C \times P \quad [1]$$

Where:

A is the computed average annual soil loss ( $\text{t ha}^{-1} \text{yr}^{-1}$ ).

R is the rainfall-runoff erosivity factor ( $\text{MJ mm ha}^{-1} \text{h}^{-1} \text{yr}^{-1}$ ).

K is the soil erodibility factor ( $\text{t h MJ}^{-1} \text{mm}^{-1}$ ).

L and S are the slope length and slope steepness factors (dimensionless), respectively, often combined as the topographic factor LS.

C is the cover management factor (dimensionless).

P is the support practice factor (dimensionless).

The analysis was performed for the years 2017 and 2024 to assess changes in soil erosion risk. All geospatial processing was implemented in Google Earth Engine (GEE) at a spatial resolution of 10 metres.

## **2.3. Data sources and processing**

### *2.3.1. Rainfall Erosivity (R-Factor)*

The R-factor was calculated using pentadal rainfall data from the Climate Hazards Group InfraRed Precipitation with Station (CHIRPS) data (Funk *et al.*, 2015). For each year, the annual precipitation total was derived by summing all pentads. The R-factor was then computed using a modified Fournier index adapted for tropical regions (Renard & Freimund, 1994):

$$R = 0.5 \times (0.073 \times P^{1.5}) \quad [2]$$

where P is the annual precipitation in mm.

### *2.3.2. Soil Erodibility (K-Factor)*

The K-factor was derived from SoilGrids 2.0 (Hengl *et al.*, 2017; Poggio *et al.*, 2021), a global soil database providing estimates of sand, silt, clay, and soil organic carbon (SOC) content at a 250m spatial resolution. The calculation was based on the EPIC model (Williams & Arnold, 1997).

Key steps included:

- a) Converting soil properties to percentages;
- b) Calculating the particle size parameter M as

$$M = (\text{silt} + \text{very fine} - \text{sand}) \times (100 - \text{clay}) \quad [3];$$

- c) Estimating soil organic matter (OM) from SOC using the van Bemmelen factor(1.72).

$$\text{Organic Matter (OM)} = \text{Soil Organic Carbon (SOC)} \times 1.72 \quad [4];$$

- d) Applying the formula:

$$K = 2.8e - 7 \times (12 - OM) \times M^{1.14} + 4.3e - 3 \times (s - 2) + 3.3e - 3 \times (p - 3) \quad [5]$$

where soil structure (s) and permeability (p) were assigned constant values typical of agricultural soils in the region.

The resulting K-factor was constrained between 0 and 0.65 to ensure physical and empirical validity and numerical stability (Wischmeier & Smith, 1958).

### 2.3.3. Topographic Factor (LS-Factor)

The LS-factor was computed from a 1-arcsecond (approx. 30m) Digital Elevation Model (DEM) sourced from the NASA SRTM global dataset.

The processing steps were:

The DEM was reprojected to UTM Zone 30N for accurate slope calculation. The slope steepness (S-factor) was calculated using a segmented function (Wischmeier & Smith, 1978):

For slopes < 9%:

$$S = 10.8 \times \sin(\theta) + 0.03 \quad [6]$$

For slopes  $\geq$  9%:

$$S = 16.8 \times \sin(\theta) - 0.5 \quad [7]$$

The slope length (L-factor) was computed using a simplified approach, assuming a constant slope length of 50 metres. The exponent M in the L-factor formula varied, and following established guidelines (McCool et al., 1987), was based on slope percent. The final LS-factor was the product of L and S.

While this study employed a well-established, GIS-based algorithm for the LS-factor, future research could explore more complex flow-routing algorithms or incorporate landform-specific refinements to potentially enhance the topographic representation of soil erosion processes.

#### *2.3.4. Cover Management (C-Factor)*

The C-factor was estimated from satellite imagery to account for vegetation cover. A Sentinel-2 surface reflectance composite was generated for the growing season (June to October) of each year to minimize cloud interference and capture the peak vegetation signal.

Vegetation index: The Transformed Soil-adjusted Vegetation Index (TSAVI) was used because of its robustness in semi-arid environments. It was calculated using the near-infrared (NIR) and red bands, with soil line parameters,  $a=1.2$ , and  $b=0.04$ , specific to semi-arid regions (Baret & Guyot, 1991).

C-factor estimation: The C-factor was derived from TSAVI using an exponential decay model (Kefi *et al.*, 2011):

$$C = \alpha \times \exp(-\beta \times TSAVI) \quad [8]$$

where  $\alpha=1.009$  and  $\beta=5.143$ . The resulting values were clamped between 0 (full protection) and 1 (bare soil).

The use of TSAVI ensured a dynamic and spatially explicit estimation of the C-factor, which is particularly robust for semi-arid environments. It is important to note that this method automatically assigns very low C-values to impervious surfaces such as built-up areas, as they exhibit spectral signatures distinct from vegetated areas or bare soil, thus correctly reflecting their lack of soil detachment by raindrop impact.

#### *2.3.5. Support Practice (P-Factor)*

The P-factor was assigned based on land use and land cover (LULC) data from the ESRI Global LULC 10m Time Series. LULC classes for each year were reclassified to P-values according to the potential for conservation practices in each class, as derived from the literature (Panagos *et al.*, 2015). The assigned values were as follows: Water (1.0), Trees (0.2), Flooded Vegetation (0.5), Crops (0.5), Built-up Area (0.9), Bare Ground (1.0), Snow/Ice (1.0), and Rangeland (0.5).

Prior to the final RUSLE calculation, all datasets were processed and harmonized to a consistent 10-metre spatial resolution within the Google Earth Engine platform. The basin boundary was used to clip all data layers, ensuring that the analysis was confined to the study area and that the edge effects were eliminated.

## **2.4. Model implementation and validation**

All factors were clipped to the boundary of the Tono Basin. The final soil loss (A) was computed by multiplying all six factor rasters, cell by cell, in GEE. The results for the individual factors and the total soil loss were exported for further analysis. The model outputs were validated by performing sanity checks on the factor values (e.g., ensuring K and C factors were within their theoretical ranges) and by comparing the spatial patterns of soil loss with known erosion-prone areas (steep slopes, bare soil) within the basin.

## **3. Results**

### **3.1. Temporal changes in soil erosion**

The analysis of soil erosion dynamics in the Tono Basin between 2017 and 2024 reveals a dramatic and statistically significant increase in erosion rates. As illustrated in Figure 2, mean soil erosion escalated from 0.846t/ha/yr in 2017 to 2.684t/ha/yr in 2024, representing a substantial 217.1% increase over the seven-year study period. This alarming trend underscores the accelerating soil degradation processes within the basin.

The magnitude of this increase is further emphasized by the total annual soil loss, which surged from approximately 8.27 million tons to 26.24 million tons, indicating a threefold increase in the absolute volume of soil displaced annually. The maximum erosion rates observed in the basin also intensified considerably, rising from 196.5t/ha/yr to 322.4t/ha/yr, suggesting the emergence of more severe localized erosion hotspots.

Statistical analysis confirmed the significance of these observed changes. A paired t-test yielded a highly significant result ( $t(999) = -24.25, p < 0.001$ ), while the non-parametric Wilcoxon signed-rank test similarly indicated strong statistical significance ( $V = 2546, p < 0.001$ ). The effect size, measured by Cohen's  $d$  of 0.767, indicated a medium to large practical significance, confirming that the observed changes are not only statistically significant but also ecologically meaningful.

The variability in erosion patterns also showed notable changes between the two periods. The coefficient of variation decreased from 158.1% in 2017 to 135.0% in 2024, suggesting a more widespread distribution of erosion risk across the basin, rather than a concentration in specific hotspots. This pattern indicates that erosion processes have become more generalized throughout the study area, potentially reflecting broader environmental changes affecting the entire basin.

The combined temporal analysis presented in Figure 2 integrates these multiple dimensions of change, providing a comprehensive visualization of the escalating erosion crisis. The consistent direction and magnitude of change across all measured parameters — mean erosion

rates, total soil loss, maximum erosion values, and statistical significance measures — collectively paint a concerning picture of rapidly deteriorating soil conservation status in the Tono Basin.

This dramatic increase in soil erosion over a relatively short seven-year period highlights the urgent need for targeted soil conservation interventions and suggests that current land management practices may be insufficient to mitigate the underlying drivers of soil degradation in the region.

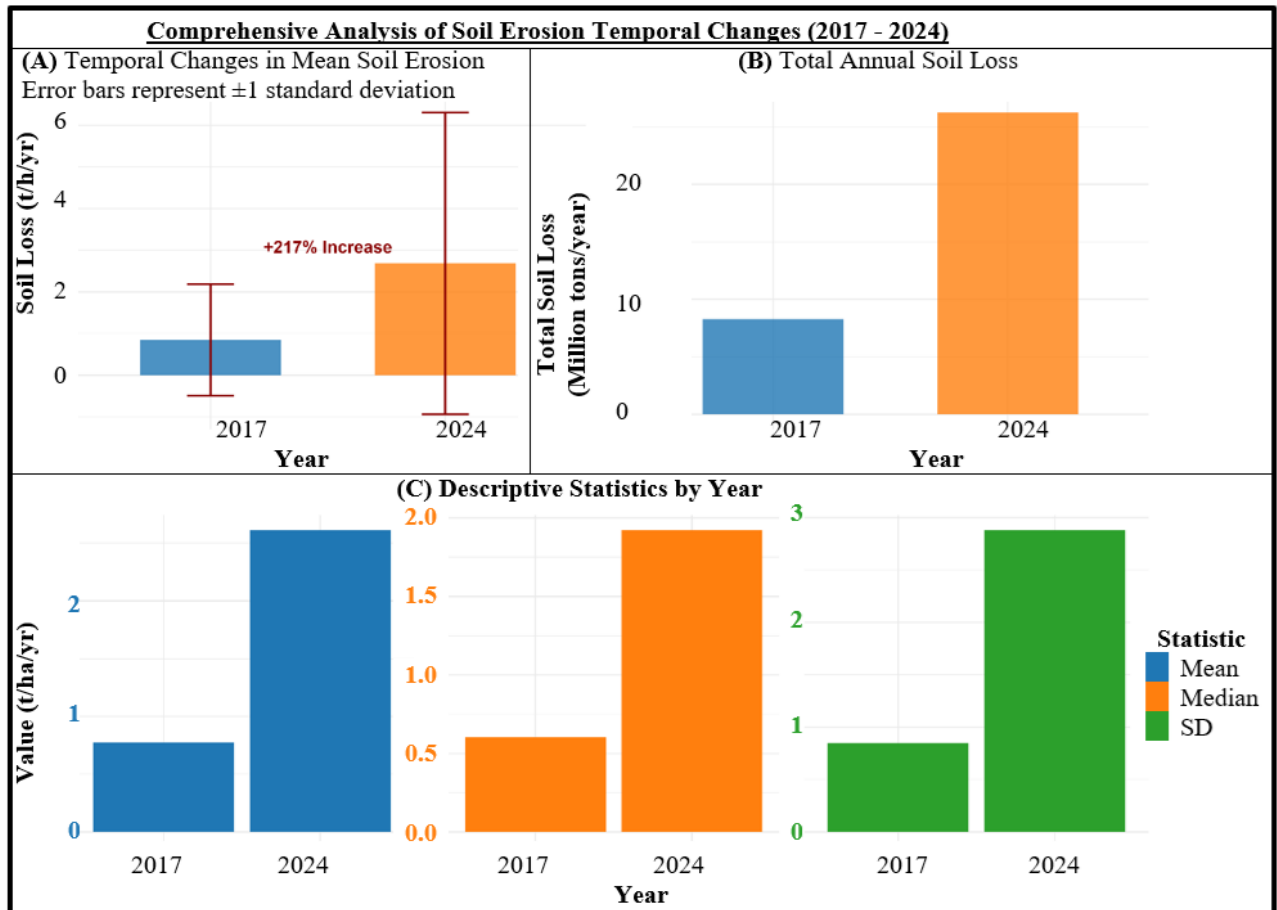


Figure 2. Comprehensive temporal analysis of soil erosion dynamics in the Tono Basin (2017-2024). The dashboard integrates (A) mean soil loss changes with error bars representing  $\pm 1$  standard deviation, (B) total annual soil loss comparison, and (C) descriptive statistics distribution, demonstrating the 217% increase in erosion rates over the study period.

### 3.2. Erosion severity classification

The classification of soil erosion into severity categories reveals a substantial transformation in the erosion risk profile of the Tono Basin between 2017 and 2024, as comprehensively illustrated in Figure 3. The analysis employed the standardized FAO/USDA erosion severity classification system, categorizing areas into six classes: Very Low (0-5t/ha/yr), Low (5-

10t/ha/yr), Moderate (10-20t/ha/yr), High (20-40t/ha/yr), Very High (40-80t/ha/yr), and Severe (>80t/ha/yr).

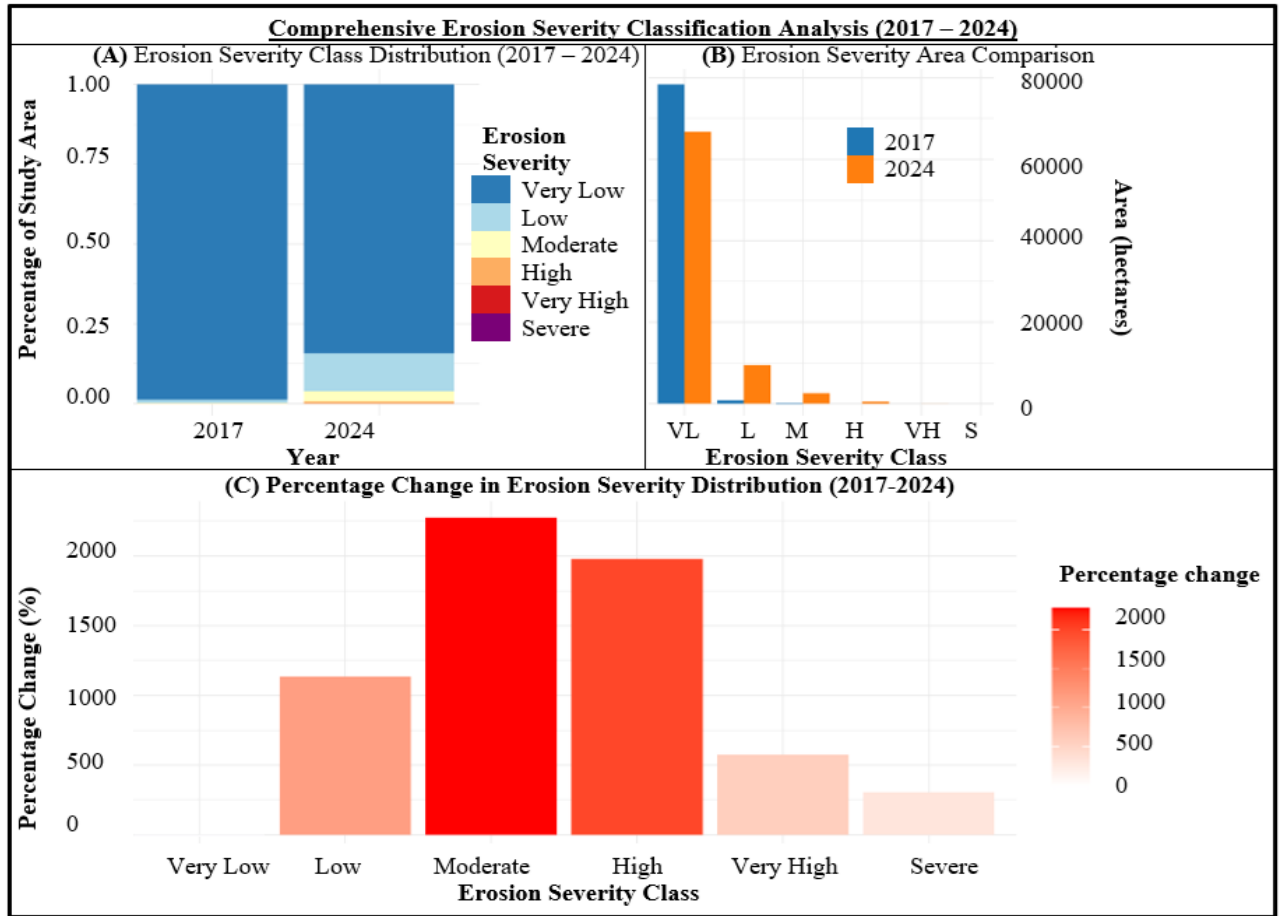


Figure 3. Comprehensive erosion severity classification analysis in the Tono Basin (2017-2024). The integrated dashboard shows (A) spatial distribution of erosion severity classes, (B) temporal changes in severity class proportions, illustrating the significant shift from 'Very Low' to higher erosion risk categories over the study period (VL=Verl Low, L=Low, M=Moderate, H=High, VH=Very High, S=Severe), and (C) percentage area coverage by severity category.

The most striking transformation observed was the dramatic reduction in areas classified as "Very Low" erosion risk, which decreased from 98.9% of the basin (78,447.7 ha) in 2017 to 84.2% (66,812.0 ha) in 2024. This 14.8 percentage point decline represents a significant shift of approximately 11,635.7 hectares from the lowest risk category to higher erosion severity classes.

Concurrently, all higher erosion risk categories exhibited exponential increases in their spatial extent. Areas experiencing "Low" severity erosion expanded remarkably from 0.97% (768.5 ha) to 11.95% (9,485.1 ha), representing a 1,134% increase. Similarly, "Moderate" erosion zones grew from 0.13% (106.1 ha) to 3.18% (2,520.2 ha), marking an extraordinary 2,276% expansion. The most severe categories showed equally concerning trends, with "High"

erosion areas increasing by 1,980%, "Very High" by 575%, and "Severe" erosion zones by 306%.

The collective area vulnerable to substantial soil degradation — encompassing the Moderate to Severe categories — expanded from a minimal 0.2% of the basin in 2017 to 3.9% in 2024. This represents a nearly 20-fold increase in high-risk erosion areas, translating to approximately 3,058.6 hectares newly classified within these concerning severity categories. While the absolute percentages of the most severe classes remain small, their exponential growth rates signal emerging erosion hotspots that warrant immediate conservation attention.

The spatial redistribution of erosion severity classes, as visualized in Figure 3, demonstrates a fundamental shift in the basin's erosion regime. The transformation from a landscape dominated by minimal erosion risk to one with substantially expanded moderate and high-risk areas indicates changing environmental conditions and land use pressures that have altered the fundamental erosion dynamics across the Tono Basin. This escalation in erosion severity underscores the urgent need for targeted soil conservation strategies, particularly in areas that transitioned into higher risk categories during the study period.

### **3.3. LULC changes and erosion relationships**

As comprehensively illustrated in Figure 4, the analysis of land use/land cover (LULC) changes and their relationship with soil erosion patterns reveals complex and often counter-intuitive dynamics in the Tono Basin between 2017 and 2024. The interplay between land cover transformations and erosion responses demonstrates that both increasing and decreasing land cover types can contribute significantly to soil degradation.

The most dramatic land use transformation was the expansion of the Built-up Area, which increased by 162.3% (+2,976.7 ha), representing the largest absolute area change among all land cover classes. This manifestation of urbanization was closely followed by substantial afforestation efforts, with Tree Cover expanding by 131.9% (+1,702.8 ha). Conversely, the most significant reduction occurred in Bare Ground which decreased by 89.6%; though, because of its minimal extent initially, this represented only 1.5 ha.

The relationship between land cover changes and erosion responses revealed several critical patterns. Built-up Area exhibited the highest absolute erosion rates for both periods, increasing from 2.43t/ha/yr to 6.14t/ha/yr (+152.8%), thereby confirming the strong erosional impact of urbanization. Similarly, Tree Cover, despite its protective reputation, showed a concerning 244.1% increase in erosion rates (from 0.25 to 0.86 t/ha/yr), thus its category as a "High Risk - Increasing" land cover, despite its substantial expansion.

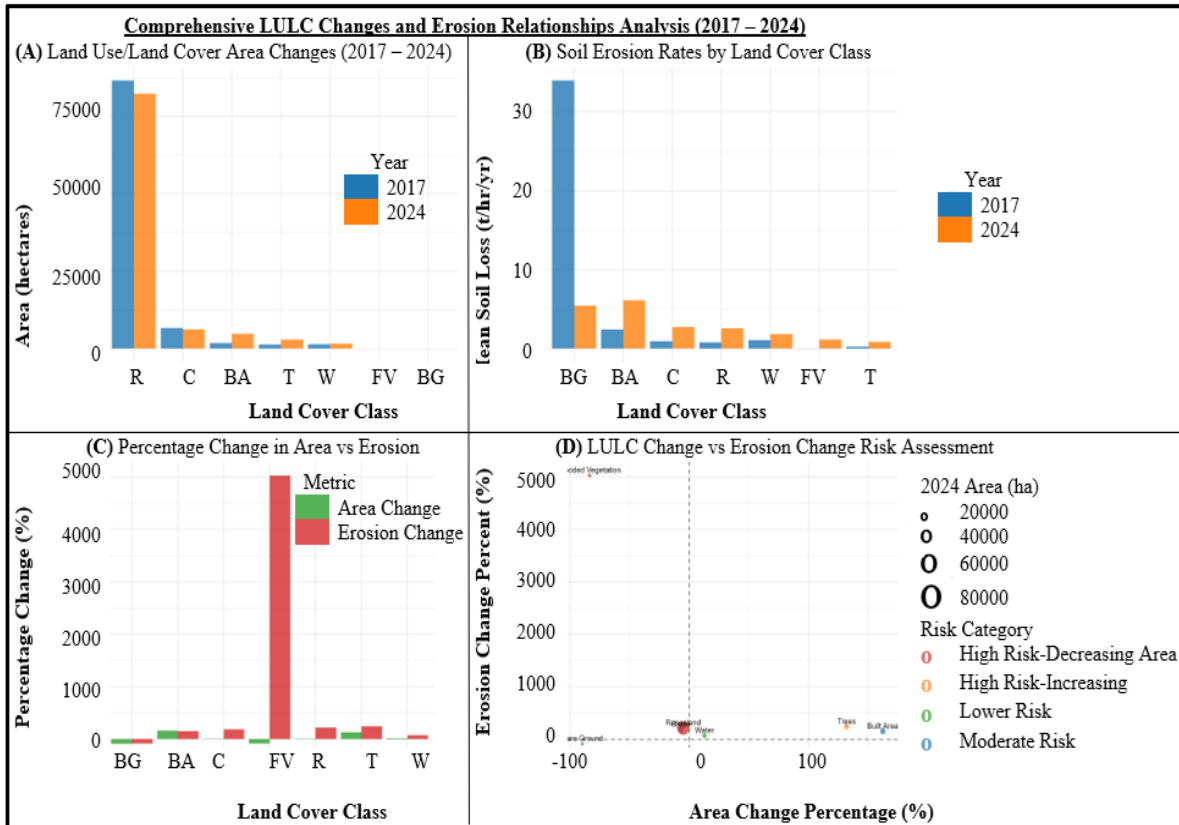


Figure 4. Integrated analysis of land use/land cover changes and erosion relationships in the Tono Basin (2017-2024). The comprehensive dashboard illustrates (A) LULC area changes across seven cover classes, (B) corresponding erosion rates by land cover type, (C) percentage changes in area *versus* erosion, and (D) a risk assessment matrix identifying high-risk categories including expanding forest areas with increasing erosion rates and vulnerable fragmented vegetation zones. [R=Rangeland, C=Crops, BA=Built Area, T=Trees, W=Water, FV=Flooded Vegetation, BG=Bare Ground].

The most extraordinary erosion response was observed in Flooded Vegetation, which experienced a staggering 5,023.7% increase in erosion rates (from 0.02 to 1.19t/ha/yr) despite an 83.6% reduction in area. This paradoxical relationship — categorized as "High Risk - Decreasing Area" — suggests that the remaining fragmented patches of flooded vegetation have become highly vulnerable to erosion processes, possibly owing to edge effects, hydrological changes, or the degradation in the quality of the remaining vegetation.

Agricultural lands showed divergent patterns: Cropland decreased by 7.1% in area but experienced a 184.7% increase in erosion rates (from 0.97 to 2.75t/ha/yr), while Rangeland, which decreased by 5.0%, saw erosion rates increase by 216.6% (from 0.81 to 2.56t/ha/yr). Both categories represent significant conservation concerns, with Rangeland classified as "High Risk - Decreasing Areas" because of the combination of area loss and dramatically increasing erosion rates.

The risk assessment matrix, as visualized in Figure 4, clearly identifies Trees as the primary high-risk category in terms of both expanding area and accelerating erosion rates. This suggests

that either the newly established forest areas are in erosion-prone locations with the tree species selected providing inadequate soil protection, or there are significant time lags in the erosion-reduction benefits of afforestation.

The complex relationships revealed in this analysis underscore the fact that simple area-based land management strategies may be insufficient for erosion control. The dramatic erosion increases in both expanding and contracting land cover categories highlight the need for targeted, spatially explicit conservation approaches that consider not only the quantity but also the quality, location, and configuration of land cover changes across the Tono Basin landscape.

### **3.4. RUSLE factor correlations**

The analysis of correlations between RUSLE factors and soil loss from 2017 to 2024 reveals critical insights into the shifting drivers of erosion in the Tono Basin. As illustrated in Figure 5, the strength and significance of relationships between soil loss and various controlling factors have undergone notable changes, highlighting an evolving erosion regime. The correlation analysis, using Pearson's correlation coefficients with significance determined at  $p < 0.05$ , illustrates the relative importance of various erosion factors throughout the seven-year study period.

The LS-factor (slope length/steepness) maintained its position as the strongest correlate with soil loss throughout the study period, strengthening from  $r = 0.674$  in 2017 to  $r = 0.756$  in 2024. This persistently strong positive correlation underscores the fundamental role of topography in influencing erosion processes in the basin that is consistent with established RUSLE principles. The increase of 0.082 in the correlation coefficient indicates that topographic influences have become even more pronounced over time, possibly because of changes in land use that have made steeper slopes more vulnerable to erosion.

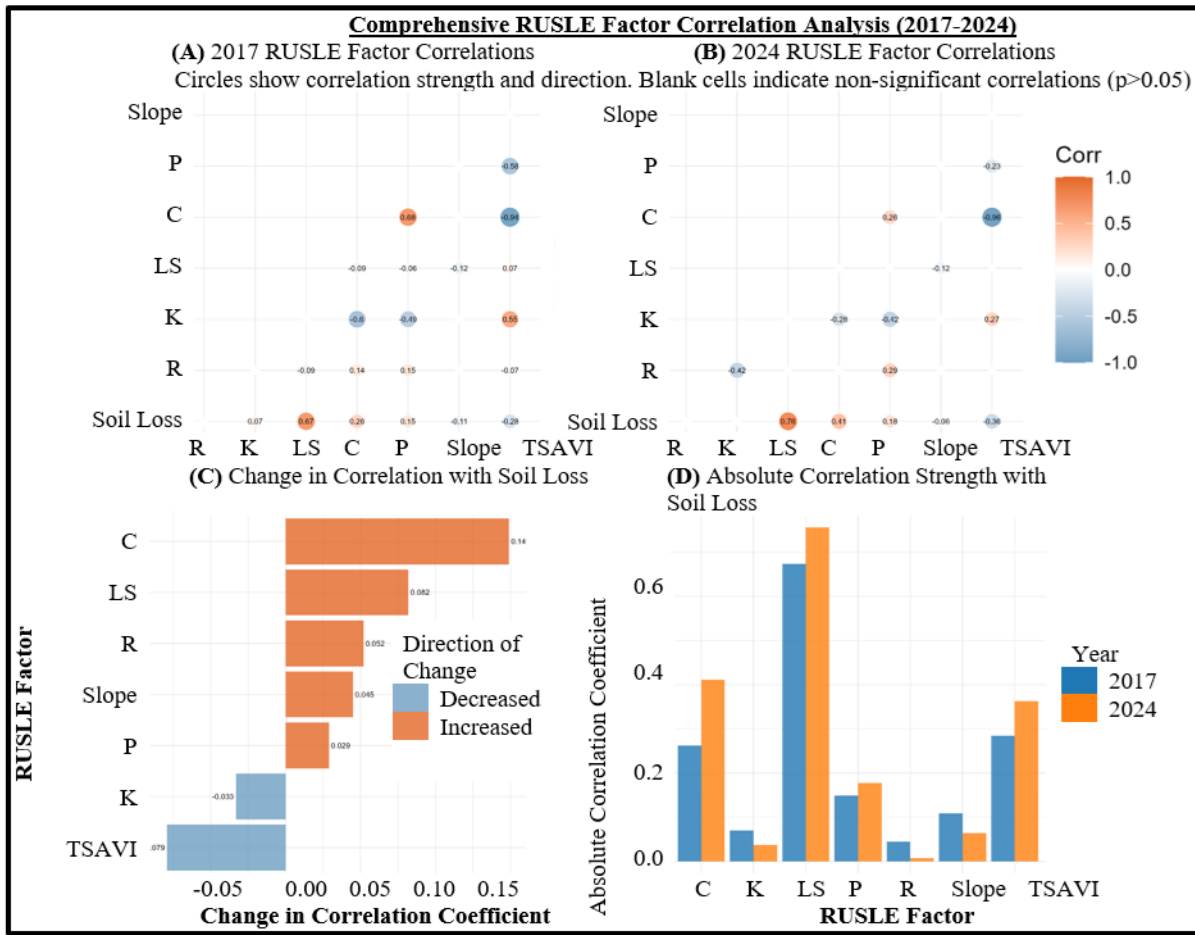


Figure 5. Comprehensive RUSLE factor correlation analysis for the Tono Basin (2017-2024). The integrated dashboard presents (A) 2017 correlation matrix showing LS-factor dominance ( $r = 0.674$ ), (B) 2024 correlations demonstrating strengthened topographic influence ( $r = 0.756$ ), (C) temporal changes in factor correlations with soil loss, and (D) comparative correlation strength analysis, revealing the increasing importance of vegetation cover factors over the study period.

The C-factor (cover management) exhibited the most substantial change in relationship strength, increasing from a moderate correlation of  $r = 0.262$  to a stronger correlation of  $r = 0.411$ . This 0.149 increase represents the largest shift among all factors and indicates that vegetation cover management practices have become increasingly important determinants of soil loss patterns in the basin. This finding aligns with research demonstrating that changes in land cover significantly influence soil erosion patterns.

The TSAVI (Transformed Soil-adjusted Vegetation Index) maintained a consistent negative correlation with soil loss, strengthening from  $r = -0.284$  to  $r = -0.363$ . This moderate negative relationship confirms the expected protective function of vegetation against erosion, with higher vegetation indices associated with reduced soil loss. The strengthening of this correlation suggests that areas with better vegetation cover became increasingly effective at mitigating erosion over time.

Other RUSLE factors demonstrated more modest influences on soil loss patterns. The P-factor (support practices) showed a slight increase in correlation from  $r = 0.149$  to  $r = 0.178$ , while the K-factor (soil erodibility) exhibited a minor decrease from  $r = 0.070$  to  $r = 0.037$ . The R-factor (rainfall erosivity) correlation remained negligible throughout the study period, shifting from  $r = -0.045$  to  $r = 0.007$ . These patterns suggest that inherent soil properties and conservation practices played relatively stable but secondary roles in determining erosion patterns compared to topographic and vegetation factors.

The temporal evolution of these correlation patterns reveals a significant shift in the primary drivers of soil erosion in the Tono Basin. The substantial strengthening of correlations for both the LS-factor and the C-factor indicates that the interaction between topography and vegetation cover has become increasingly deterministic in shaping erosion patterns. This finding has important implications for targeted conservation planning, suggesting that interventions focusing on strategic vegetation management in topographically sensitive areas may yield the greatest erosion reduction benefits.

### **3.5. Spatial patterns and hotspots**

As comprehensively illustrated in Figure 6, the spatial analysis of soil erosion in the Tono Basin reveals distinct clustering patterns and the emergence of well-defined erosion hotspots between 2017 and 2024. The integration of hotspot classification and spatial autocorrelation analysis provides critical insights into the spatial organization of erosion processes across the basin.

Spatial autocorrelation analysis using Global Moran's I demonstrated significant clustering of soil erosion values in both study periods. The Moran's I statistic increased from 0.189 in 2017 ( $p < 0.001$ ) to 0.259 in 2024 ( $p < 0.001$ ), indicating a strengthening of spatial clustering patterns over time. This substantial increase in spatial autocorrelation suggests that erosion processes became more concentrated and spatially organized, with high-erosion areas becoming increasingly aggregated in specific portions of the landscape.

Hotspot analysis classified the basin into four distinct categories based on erosion persistence and emergence. Persistent hotspots, representing areas that consistently experienced above-average erosion in both periods, accounted for 24.3% of the study area. These zones represent the most critical areas requiring immediate conservation interventions, as they demonstrate sustained vulnerability to soil degradation. New hotspots, covering 10.8% of the basin, represent emerging risk areas where erosion intensities crossed the threshold between 2017 and 2024, signalling locations where recent environmental changes or land use practices may be exacerbating soil loss.

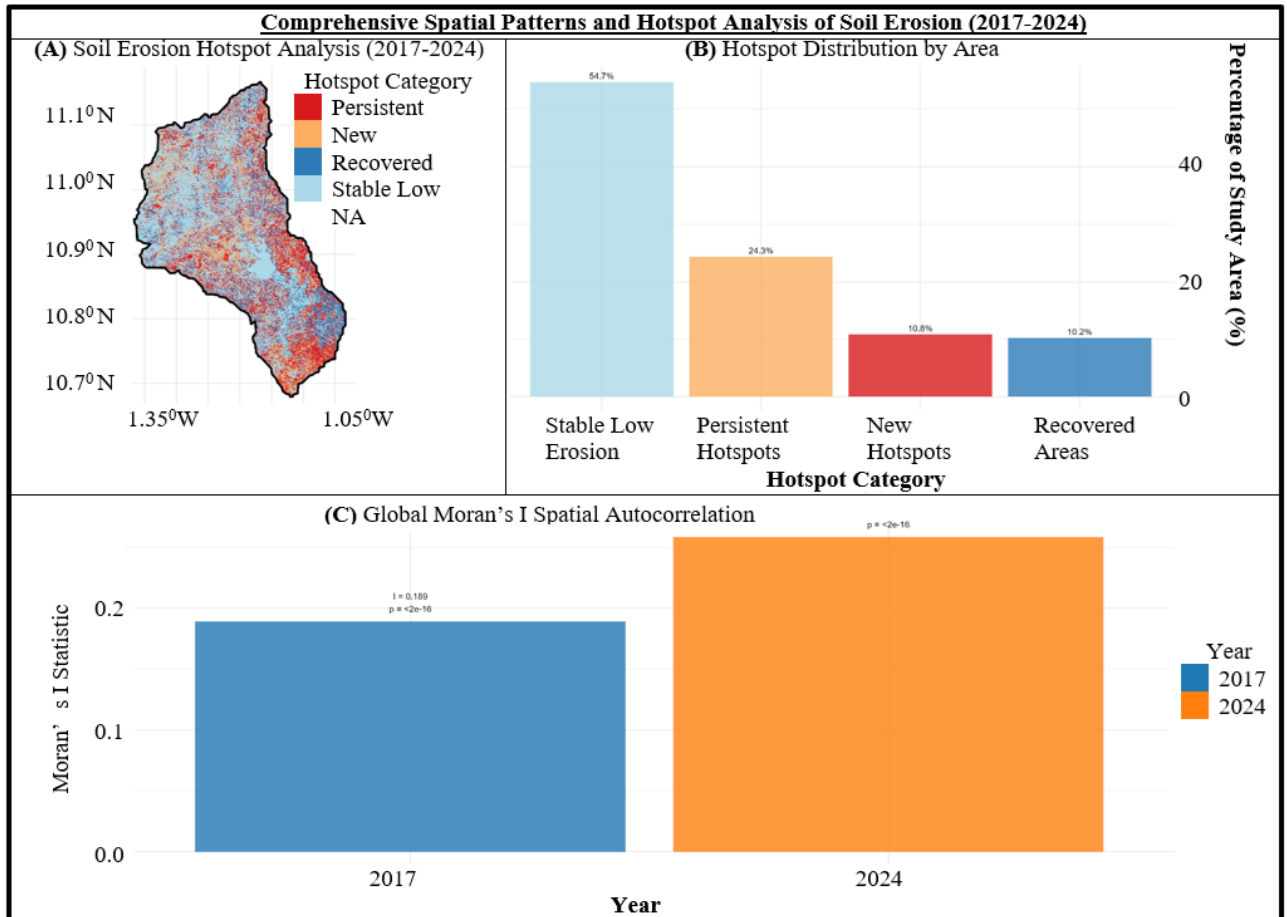


Figure 6. Comprehensive spatial patterns and hotspot analysis of soil erosion in the Tono Basin (2017-2024). The integrated dashboard presents (A) spatial distribution of erosion hotspot categories, (B) areal percentage of persistent hotspots (24.3%), new hotspots (10.8%), recovered areas (10.2%), and stable zones (54.7%), and (C) Global Moran's I spatial autocorrelation showing significantly increasing clustering strength from 0.189 to 0.259, indicating enhanced spatial organization of erosion patterns over time.

The analysis also identified recovered areas (10.2% of the basin) where erosion levels decreased from above to below the mean threshold, potentially indicating successful conservation outcomes or beneficial land use changes. The larger part of the basin (54.7%) maintained stable low erosion conditions throughout the study period, representing areas with inherent resilience or subject to effective ongoing soil conservation practices.

The spatial organization of these hotspot categories, combined with the significant autocorrelation patterns, underscores the non-random distribution of erosion risk across the Tono Basin. The concentration of erosion in specific areas suggests underlying environmental controls, such as topographic features, soil characteristics, or land use patterns, that consistently influence erosion susceptibility. These findings emphasize the importance of spatially targeted conservation strategies that recognize the clustered nature of erosion risk and prioritize interventions in areas exhibiting persistent or emerging hotspot characteristics.

## **4. Discussion**

### **4.1. Synthesis of key findings**

The comprehensive soil erosion assessment conducted in the Tono Basin between 2017 and 2024 reveals a concerning acceleration of soil degradation processes, with mean erosion rates increasing by 217.1% from 0.85t/ha/yr to 2.68t/ha/yr. This dramatic escalation represents one of the most rapid soil erosion increases documented in comparable semi-arid watersheds and signals the crossing of a critical environmental threshold. The total annual soil loss surged from 8.27 million tons to 26.24 million tons, indicating substantial off-site impacts on water quality, reservoir sedimentation, and agricultural productivity downstream. This finding is particularly critical as studies in northern Ghana have shown that reservoir catchments with similar soils (Lixisols, Fluvisols) are prone to sedimentation, which reduces water storage capacity and the designated reservoir life (Adongoa *et al.*, 2019). The severity of this loss is underscored by research in Ghana's Upper East Region, where soil erosion directly impacts crop production, food security, and livelihoods, with sedimentation exacerbating the decline in agricultural productivity (Sodoke *et al.*, 2025).

The severity classification analysis demonstrates a fundamental shift in the basin's erosion regime, with areas experiencing "Very Low" erosion risk declining from 98.9% to 84.2% of the basin, while moderate to severe erosion categories expanded nearly 20-fold from 0.2% to 3.9%. This redistribution reflects a landscape-scale transformation where erosion processes have become more widespread and intense, particularly in topographically sensitive and land-use transition zones. Similar spatial targeting of soil loss has been emphasized as crucial for cost-effective mitigation, allowing for the implementation of conservation practices in critical areas for optimal impact (Dumedah & Evans Kyeremanteng, 2019). This approach is vital, as seen in the Asutifi North District, where a significant proportion of soil loss was attributed to severe and very high erosion classes, necessitating targeted interventions (OSEI-GYABAAH *et al.*).

### **4.2. Land use change dynamics and erosion responses**

The complex relationships between land use changes and erosion responses reveal several paradoxical patterns that challenge conventional erosion control assumptions. The substantial afforestation efforts, evidenced by a 131.9% increase in tree cover, are associated with a 244.1% increase in erosion rates within these areas. This counter-intuitive finding suggests several potential mechanisms: the newly established plantations might have exposed their soils during the establishment phase, the selected tree species might not have been able to provide adequate groundcover protection, or afforestation might have been concentrated on erosion-prone slopes where the mere attempt to establish a vegetation cover would be considered challenging. This aligns with the "afforestation-erosion paradox" observed in other regions. For instance, while forests generally protect the soil, the type of vegetation and how it is

managed are critical issues. In the Chisheke watershed, for instance, well-established forests recorded low soil losses ( $6.5 \text{ t ha}^{-1} \text{ yr}^{-1}$ ), whereas poorly managed or newly established vegetative cover offered less protection (Chuma *et al.*, 2022). The critical role of vegetation structure is further highlighted by evapotranspiration studies in the Tono Basin which found that a decrease in Leaf Area Index (LAI) for all major vegetation types between 2009 and 2017 led to sparser canopies (Alhassan & Jin, 2020). Such a reduction in LAI diminishes the protective cover of the vegetation against rainfall impact and can increase the area of soil exposure, potentially explaining the heightened erosion in some newly vegetated areas.

The most dramatic erosion response occurred in flooded vegetation areas, which experienced a staggering 5,023.7% increase in erosion rates despite an 83.6% reduction in area. This extreme vulnerability of the remaining fragmented patches highlights the importance of ecosystem connectivity in erosion control and suggests that habitat fragmentation may have compromised the protective function of these riparian zones. The expansion of built-up areas by 162.3%, coupled with a 152.8% increase in their erosion rates, confirms the significant impact of urbanization in sediment generation. This is consistent with findings from the Lafa Basin study in Ghana, where urbanization pressures were identified as key drivers of erosion, and from the Chisheke watershed study, where settlements exhibited the highest average soil losses ( $65 \text{ t ha}^{-1} \text{ yr}^{-1}$ ) (Chuma *et al.*, 2022; Mantey & Aduah, 2020). Furthermore, the conversion of vegetated lands to built-up areas, as observed in the Upper East Region, is a well-documented driver that increases soil exposure and erosion risk (Sodoke *et al.*, 2025). This is consistent with land cover analyses in the Tono Basin, which showed an increase in built-up area from 1.47% to 2.41% between 2009 and 2017.

#### **4.3. Changing erosion drivers and factor interactions**

The RUSLE factor correlation analysis reveals evolving erosion dynamics, with topographic factors (LS-factor) maintaining their primacy ( $r = 0.756$  in 2024) while vegetation-related factors substantially increased in importance. The cover management factor (C-factor) exhibited the largest correlation increase (+0.149), indicating that vegetation cover has become a more critical determinant of erosion patterns over time. This shift suggests that as land use intensification progresses, the protective function of vegetation becomes increasingly vital in moderating erosion processes. The use of NDVI to derive the C-factor, as demonstrated in multiple studies, effectively captures the spatial variability in vegetation cover and its impact on erosion (Dumedah & Evans Kyeremanteng, 2019). This is corroborated by sensitivity analyses in the Upper East Region, which identified the C-factor as one of the most profound and significant predictors of soil loss (Sodoke *et al.*, 2025). The growing importance of vegetation cover is supported by energy balance studies in the Tono Basin which demonstrate that land cover type significantly controls the partitioning of net radiation into latent heat (LE) and sensible heat (H) fluxes (Alhassan & Jin, 2020). Changes in this partitioning, driven by

vegetation changes, directly affect the energy available for driving evapotranspiration and, by extension, influence soil moisture conditions and erosion susceptibility.

The strengthening negative correlation between TSAVI and soil loss ( $r = -0.363$  in 2024) confirms the expected protective role of vegetation while highlighting its growing importance in the evolving erosion regime. The minimal influence of rainfall erosivity (R-factor) throughout the study period suggests that intrinsic landscape characteristics rather than precipitation patterns are the dominant controls in the spatial distribution of erosion in the Tono Basin. This finding concurs with studies in northern Ghana, which also classified rainfall as only "moderately erosive," with topography and land cover being more significant drivers of soil loss patterns (Adongoa et al., 2019). This is further supported by the regression analysis of the Upper East Region, where, unlike slope, cover management, and support practices, rainfall erosivity was found not to be a statistically significant predictor of soil loss (Sodoke *et al.*, 2025). This is further evidenced by the work of (Alhassan & Jin, 2020) in the same basin, who found that despite an overall increase in net radiation ( $R_n$ ) and latent heat flux (LE) between 2009 and 2017 — which would influence the energy available for erosive processes — the spatial patterns of these fluxes were fundamentally dictated by land cover and not by uniform climatic forcing.

#### **4.4. Spatial organization and hotspot dynamics**

Spatial analysis of the relevant variables in this study reveals increasingly organized erosion patterns, with Moran's I values increasing from 0.189 to 0.259, indicating stronger spatial clustering of high-erosion areas. This enhanced spatial organization suggests that erosion processes are becoming more focused in specific landscape positions, potentially reflecting the increasing influence of localized factors such as land management practices, topographic convergence, or soil characteristics. The methodology of using GIS-based RUSLE is particularly powerful in visualizing and identifying these spatial patterns and critical risk hotspots.

The identification of persistent hotspots (24.3% of the basin) provides critical guidance for targeted conservation interventions. The substantial portion of the basin maintaining stable low erosion conditions (54.7%) demonstrates that significant areas retain their natural resilience or benefit from effective conservation practices. This underscores the value of spatial targeting, since implementing measures across the entire basin would be inefficient. In fact, focusing on the 24.3% of persistent hotspots and the 10.8% of new hotspots would yield the greatest returns on investments for soil conservation (Dumedah & Evans Kyeremanteng, 2019). This approach is echoed in the Asutifi North District, where the generated soil erosion risk map serves as a roadmap for decision-makers to prioritize areas for soil conservation interventions (OSEI-GYABAAH et al.). This targeted approach is crucial in a basin such as the Tono, where research has shown significant spatial heterogeneity in the key hydrological processes (e.g.,

evapotranspiration) across the different land cover types (Alhassan & Jin, 2020), thereby implying that erosion controls will also need to be spatially tailored.

#### **4.5. Management implications and conservation priorities**

The findings necessitate a paradigm shift in soil conservation strategies for the Tono Basin, moving from generalized approaches to spatially targeted interventions that address the specific erosion processes identified in this study. Priority should be given to the following interventions:

**Persistent Hotspot Intervention:** Implement reinforced conservation measures in the identified hotspots, focusing on structural controls and vegetative stabilization tailored to local conditions. Practices such as contour ploughing, and stone/earth binding have been recognized as effective measures to reduce soil loss in agricultural catchments (Adongoa *et al.*, 2019; Chuma *et al.*, 2022).

**Afforestation Strategy Reform:** Re-evaluate afforestation programmes to ensure species selection, planting density, and spatial distribution to optimize the benefits of erosion control, particularly during the establishment phases. Learning from the Chisheke watershed, the promotion of permanent crops such as tea plantations can provide excellent forms of groundcover and significantly reduce erosion (Chuma *et al.*, 2022). This is critical as the C-factor has been shown to be a dominant factor controlling soil loss (Sodoke *et al.*, 2025). The selection of species should aim to rapidly achieve a high Leaf Area Index (LAI), as LAI is a key biophysical control on surface energy fluxes and soil moisture retention in the Tono Basin (Alhassan & Jin, 2020).

**Riparian Zone Protection:** Enhance the protection and restoration of the remaining flooded vegetation areas, recognizing their disproportionate importance in erosion control. Education on protecting the riparian area and prohibiting farming practices in these buffer zones is crucial to mitigate their fragmentation and degradation (Adongoa *et al.*, 2019; Chuma *et al.*, 2022).

**Urban Erosion Management:** Develop integrated sediment control measures for expanding built-up areas. As demonstrated in the Lafa Basin, the absence of a vegetation cover (high C-factor) in urban areas greatly exacerbates erosion, necessitating the implementation of proper land use planning and a green infrastructure (Mantey & Aduah, 2020).

**Agricultural Conservation:** Strengthen soil conservation practices in croplands, where despite slight area reductions, erosion rates have increased substantially. Adopting support practices (P-factor) such as contour farming across slopes can significantly reduce the P-factor value from 1.0 to lower values, thereby directly reducing soil loss (Adongoa *et al.*, 2019). The significant role of the P-factor in mitigating soil loss, as confirmed by regression analysis (Sodoke *et al.*, 2025), underscores the importance of promoting Good Agricultural Practices

(GAP) such as cover cropping and reduced tillage to reduce soil exposure (OSEI-GYABAAH et al.; Sodoke et al., 2025).

#### **4.6. Methodological Considerations and Research Needs**

The RUSLE-GIS integration employed in this study provides a robust framework for spatial erosion assessment. The sensitivity of the model to topographic and vegetation factors aligns with the established erosion theory, but the dynamic interactions between factors highlight the need for process-based models that can capture non-linear responses to land use changes.

Future research should prioritize: (1) high-temporal resolution monitoring to capture seasonal and event-based erosion dynamics; (2) field validation of model predictions to quantify estimation uncertainties, a step that strengthens the reliability of the GIS-based approach (Chuma *et al.*, 2022); (3) investigation of the afforestation-erosion paradox through detailed soil and vegetation studies; and (4) assessment of climate change impacts on future erosion trajectories, particularly as rainfall erosivity is a key RUSLE factor. Future studies should also seek to integrate soil erosion models with surface energy balance models. Combining RUSLE with sophisticated evapotranspiration estimates, such as those derived from the Two-source Energy Balance (TSEB) model validated for the Tono Basin (Alhassan & Jin, 2020), could provide for a more holistic understanding of the coupled water and sediment cycles, improving predictions of how changes in land cover and climate jointly affect soil loss.

Furthermore, while the use of SoilGrids 2.0 provided a consistent and globally available dataset for estimating soil erodibility, the inherent uncertainty and spatial resolution (250m) of this product remain a limitation. Future studies aiming for higher precision could benefit from region-specific, high-resolution soil surveys to better characterize the spatial variability of the K-factor within the basin.

## **5. Conclusion**

This comprehensive study demonstrates the critical escalation of soil erosion in the Tono Basin between 2017 and 2024, thereby revealing a landscape undergoing rapid environmental transformation. The 217.1% increase in mean erosion rates and the substantial expansion of moderate to severe erosion categories from 0.2% to 3.9% of the basin area underscore the urgent need for intervention. The integration of RUSLE modeling with spatial statistics has provided unprecedented insights into the dynamics and patterns of soil degradation in this semi-arid watershed.

The research successfully identified the complex interplay of factors driving erosion intensification, with topography maintaining its primacy, while vegetation cover factors gained increasing importance over time. The paradoxical relationships observed — particularly the

increased erosion in expanding forested areas and the extreme vulnerability of fragmented flooded vegetation — challenge conventional erosion control assumptions and highlight the need for contextually specific conservation strategies. The spatial clustering of erosion patterns, evidenced by the strengthening Moran's I values and the identification of persistent and emerging hotspots, provides a robust scientific basis for targeted intervention.

The methodological framework developed in this study, combining traditional erosion modeling with advanced spatial analysis and temporal change detection, offers a replicable approach for similar assessments in comparable semi-arid regions. The findings not only contribute to the scientific understanding of erosion dynamics in rapidly changing landscapes, but also provide practical guidance for resource managers and policymakers.

Looking forward, the implementation of spatially targeted conservation measures addressing the identified hotspot areas, coupled with revised afforestation strategies and the enhanced protection of vulnerable ecosystems, offers the potential to reverse current degradation trends. Future research should focus on high-resolution temporal monitoring, field validation of model predictions, and the development of adaptive management frameworks that can respond to the evolving erosion regime documented in this study. The preservation of the Tono Basin's soil resources requires immediate, evidence-based action, informed by the patterns and processes revealed through this comprehensive assessment.

## **6. References**

- Abdelsamie, E. A., Abdellatif, M. A., Hassan, F. O., El Baroudy, A. A., Mohamed, E. S., Kucher, D. E., & Shokr, M. S. (2022). Integration of RUSLE model, remote sensing and GIS techniques for assessing soil erosion hazards in arid zones. *Agriculture*, *13*(1), 35.
- Adongoa, T., Agyare, W., Abagalec, F., & Kyei-Baffour, N. (2019). Spatial soil loss estimation using an integrated GIS-based revised universal soil loss equation (RUSLE) in selected watersheds in northern Ghana. *International Journal of Engineering, Science and Technology*, *11*(4), 58-74.
- Alhassan, A., & Jin, M. (2020). Evapotranspiration in the Tono Reservoir Catchment in Upper East Region of Ghana Estimated by a Novel TSEB Approach from ASTER Imagery. *Remote Sensing*, *12*(3), 569. <https://www.mdpi.com/2072-4292/12/3/569>
- Bai, Z., Dent, D. L., Olsson, L., & Schaeppman, M. E. (2008). Global assessment of land degradation and improvement 1. Identification by remote sensing. *Report*, 2008.
- Baret, F., & Guyot, G. (1991). Potentials and limits of vegetation indices for LAI and APAR assessment. *Remote sensing of environment*, *35*(2-3), 161-173.
- Borrelli, P., Robinson, D. A., Fleischer, L. R., Lugato, E., Ballabio, C., Alewell, C., Meusburger, K., Modugno, S., Schütt, B., & Ferro, V. (2017). An assessment of the global impact of 21st century land use change on soil erosion. *Nature communications*, *8*(1), 2013.
- Brown, L. R. (2019). The worldwide loss of cropland. In *Future Dimensions of World Food and Population* (pp. 57-96). CRC Press.
- Chuma, G. B., Bora, F. S., Ndeko, A. B., Mugumaarhahama, Y., Cirezi, N. C., Mondo, J. M., Bagula, E. M., Karume, K., Mushagalusa, G. N., & Schimtz, S. (2022). Estimation of soil erosion using

- RUSLE modeling and geospatial tools in a tea production watershed (Chisheke in Walungu), eastern Democratic Republic of Congo. *Modeling Earth Systems and Environment*, 8(1), 1273-1289.
- Dumedah, G., & Evans Kyeremanteng, D. E. (2019). Spatial targeting of soil loss using RUSLE in GIS: the case of Asokore Mampong municipality, Ghana. *GEOSPATIAL INFORMATION*, 3(1).
- Funk, C., Peterson, P., Landsfeld, M., Pedreros, D., Verdin, J., Shukla, S., Husak, G., Rowland, J., Harrison, L., & Hoell, A. (2015). The climate hazards infrared precipitation with stations—a new environmental record for monitoring extremes. *Scientific data*, 2(1), 1-21.
- Ganasri, B., & Ramesh, H. (2016). Assessment of soil erosion by RUSLE model using remote sensing and GIS-A case study of Nethravathi Basin. *Geoscience Frontiers*, 7(6), 953-961.
- Ghosh, A., Rakshit, S., Tikle, S., Das, S., Chatterjee, U., Pande, C. B., Alataway, A., Al-Othman, A. A., Dewidar, A. Z., & Mattar, M. A. (2022). Integration of GIS and remote sensing with RUSLE model for estimation of soil erosion. *Land*, 12(1), 116.
- Gorelick, N., Hancher, M., Dixon, M., Ilyushchenko, S., Thau, D., & Moore, R. (2017). Google Earth Engine: Planetary-scale geospatial analysis for everyone. *Remote sensing of environment*, 202, 18-27.
- Hengl, T., Mendes de Jesus, J., Heuvelink, G. B., Ruiperez Gonzalez, M., Kilibarda, M., Blagotić, A., Shanguan, W., Wright, M. N., Geng, X., & Bauer-Marschallinger, B. (2017). SoilGrids250m: Global gridded soil information based on machine learning. *PloS one*, 12(2), e0169748.
- Kefi, M., Yoshino, K., Setiawan, Y., Zayani, K., & Boufaroua, M. (2011). Assessment of the effects of vegetation on soil erosion risk by water: a case of study of the Batta watershed in Tunisia. *Environmental Earth Sciences*, 64(3), 707-719.
- Lal, R. (2001). Soil degradation by erosion. *Land degradation & development*, 12(6), 519-539.
- Mantey, S., & Aduah, M. S. (2020). Determination of Soil Erosion Vulnerability in the Lafa Basin of Ghana using RUSLE and GIS. *International Journal of Engineering Research and Technology*, 9(1), 247-254.
- Mccool, D. K., Brown, L. C., Foster, G., Mutchler, C., & Meyer, L. (1987). Revised slope steepness factor for the Universal Soil Loss Equation. *Transactions of the ASAE*, 30(5), 1387-1396.
- Nkrumah, F., Vischel, T., Panthou, G., Klutse, N. A. B., Adukpo, D. C., & Diedhiou, A. (2019). Recent trends in the daily rainfall regime in southern West Africa. *Atmosphere*, 10(12), 741.
- Nyamekye, C., Thiel, M., Schönbrodt-Stitt, S., Zoungrana, B. J.-B., & Amekudzi, L. K. (2018). Soil and water conservation in Burkina Faso, west Africa. *Sustainability*, 10(9), 3182.
- OSEI-GYABAAH, A. P., Addo, S., & Osei, P. Mapping Soil Erosion Risk Using Rusle Model and its Effects on Agricultural Lands in Asutifi North District, Ahafo Region, Ghana: Implications for Sustainable Agricultural Production. *Ahafo Region, Ghana: Implications for Sustainable Agricultural Production*.
- Panagos, P., Borrelli, P., Poesen, J., Ballabio, C., Lugato, E., Meusburger, K., Montanarella, L., & Alewell, C. (2015). The new assessment of soil loss by water erosion in Europe. *Environmental science & policy*, 54, 438-447.
- Poggio, L., De Sousa, L. M., Batjes, N. H., Heuvelink, G. B., Kempen, B., Ribeiro, E., & Rossiter, D. (2021). SoilGrids 2.0: producing soil information for the globe with quantified spatial uncertainty. *Soil*, 7(1), 217-240.
- Renard, K. G. (1997). *Predicting soil erosion by water: a guide to conservation planning with the Revised Universal Soil Loss Equation (RUSLE)*. US Department of Agriculture, Agricultural Research Service.
- Renard, K. G., & Freimund, J. R. (1994). Using monthly precipitation data to estimate the R-factor in the revised USLE. *Journal of hydrology*, 157(1-4), 287-306.

- Sodoke, S., Andam-Akorful, S. A., Amuah, E. E. Y., Amoah, E. G., Anokye, K., Nang, D. B., & Kazapoe, R. W. (2025). GIS-based assessment of soil erosion impact and mitigation strategies for sustainable agriculture in Ghana's most vulnerable region. *Environmental and Sustainability Indicators*, 25, 100551.
- Tamene, L., & Le, Q. B. (2015). Estimating soil erosion in sub-Saharan Africa based on landscape similarity mapping and using the revised universal soil loss equation (RUSLE). *Nutrient cycling in agroecosystems*, 102(1), 17-31.
- Vrieling, A. (2006). Satellite remote sensing for water erosion assessment: A review. *Catena*, 65(1), 2-18.
- Williams, J., & Arnold, J. (1997). A system of erosion—sediment yield models. *Soil technology*, 11(1), 43-55.
- Wischmeier, J., & Smith, S. (1958). Universal soil loss equation.
- Wischmeier, W. H., & Smith, D. D. (1978). *Predicting rainfall erosion losses: a guide to conservation planning*. Department of Agriculture, Science and Education Administration.